Journal of Cleaner Production 386 (2023) 135836

Contents lists available at ScienceDirect

Journal of Cleaner Production

journal homepage: www.elsevier.com/locate/jclepro

Bio-based lacquers from industrially processed tomato pomace for sustainable metal food packaging

José J. Benítez [a,**], María C. Ramírez-Pozo [b], María M. Durán-Barrantes [b], Antonio Heredia [c], Giacomo Tedeschi [d], Luca Ceseracciu [e], Susana Guzman-Puyol [f], David Marrero-López [g], Alessandro Becci [h], Alessia Amato [h], José A. Heredia-Guerrero [f,*]

[a] Instituto de Ciencia de Materiales de Sevilla, Centro mixto CSIC-Universidad de Sevilla, Americo Vespucio 49, Isla de la Cartuja, Sevilla, 41092, Spain
[b] Departamento de Ingeniería Química, Escuela Politécnica Superior, Universidad de Sevilla, Virgen de África 7, 41011, Sevilla, Spain
[c] Instituto de Hortofruticultura Subtropical y Mediterránea "La Mayora", Universidad de Málaga-Consejo Superior de Investigaciones Científicas (IHSM, UMA-CSIC), Departamento de Biología Molecular y Bioquímica, Facultad de Ciencias, E-29071, Málaga, Spain
[d] Smart Materials, Istituto Italiano di Tecnologia, Via Morego 30, 16163, Genova, Italy
[e] Materials Characterization Facility, Istituto Italiano di Tecnologia, Via Morego 30, 16163, Genova, Italy
[f] Instituto de Hortofruticultura Subtropical y Mediterránea "La Mayora", Universidad de Málaga-Consejo Superior de Investigaciones Científicas (IHSM, UMA-CSIC), Bulevar Louis Pasteur, 49, 29010, Málaga, Spain
[g] Universidad de Málaga, Departamento de Física Aplicada I, 29071, Málaga, Spain
[h] Department of Life and Environmental Sciences-DiSVA, Università Politecnica delle Marche, Via Brecce Bianche, 60131, Ancona, Italy

ARTICLE INFO

Handling Editor: Meisam Tabatabaei

Keywords:
Bio-based lacquer
Food canning
Tomato pomace
Circular bioeconomy
Life cycle analysis
Metal packaging

ABSTRACT

Bio-based lacquers prepared from an underutilized tomato processing residue such as pomace have been investigated as sustainable alternatives to bisphenol A (BPA)-based coatings for metal food packaging. The fabrication methodology consisted of a two-step process: spray-coating of a paste of the lipid fraction of tomato pomace with a mixture ethanol:H_2O (3:1, v:v) on common metal substrates, used for food canning, such as aluminum (Al), chromium-coated tin-free steel (TFS), and electrochemically tin-plated steel (ETP), followed by the self melt-polycondensation of such lipid fraction. The polymerization reaction was conducted at 200 °C for different times (10, 20, 30, 40, 50, and 60 min) and was monitored by specular infrared spectroscopy, resulting in maximum degrees of esterification of ~92% for Al and ~85% for TFS and ETP substrates. The anticorrosion performance of the coatings was studied by electrochemical impedance spectroscopy at different immersion times (time intervals of 2–5 h during an overall stability test up to 170 h) in an aqueous solution of 1 wt% NaCl. The degree of polymerization and the physical properties of the coatings showed a strong dependence on the metal substrate used. In general, the best results were found for tomato pomace-based lacquers applied on aluminum, achieving higher mechanical strength (critical load of 1739 ± 198 mN for Al, 1078 ± 31 mN for ETP, and 852 ± 206 mN for TFS), hydrophobicity (water contact angle ~95° for Al, ~91° for ETP, and ~88° for TFS), and improved anticorrosion performance (coating resistance of 0.7 MΩcm^2 after 170 h of immersion for Al, 0.7 MΩcm^2 after 70 h of immersion for TFS, and negligible coating resistance for ETP). In view of the technical innovation proposed in the present paper, the estimation of the environmental sustainability of the process has been considered relevant to fit the circular economy target. For this purpose, a life cycle analysis (LCA) was applied to the overall process, revealing multiple advantages for both the environment and human health.

1. Introduction

Common, non-renewable plastics from fossil resources are ubiquitous materials that can be found in almost all everyday commodities. In fact, the worldwide annual petroleum-based plastic production is ~360 Mt, a value that is a serious threat to the environment, if one considers their persistence in marine and terrestrial ecosystems, their presence as microplastics and the release of toxic components in the food chain as

* Corresponding author.
** Corresponding author.
E-mail addresses: benitez@icmse.csic.es (J.J. Benítez), ja.heredia@csic.es (J.A. Heredia-Guerrero).

https://doi.org/10.1016/j.jclepro.2022.135836
Received 10 October 2022; Received in revised form 14 December 2022; Accepted 30 December 2022
Available online 31 December 2022

well as the high environmental impact of fossil resources extraction and processing (Otoni et al., 2021; PlasticsEurope, 2021). Data from 2020 report that, in Europe, ~40.5% of plastics were used for packaging (mostly food packaging), mainly for single-use products with short service life and thrown away in a linear "take-make-dispose" economy model (PlasticsEurope, 2021). Moreover, due to the growing population of our planet and the consequent higher demand for convenience foods in urban areas, an increasing production of food packaging materials is expected. In this regard, it is important to emphasize that the use of food packaging is essential for transporting, storing, handling, and preserving food by increasing its shelf life while safely keeping its nutritional value and organoleptic properties.

Metal packaging plays a key role protecting canned food against physical, chemical, and microbiological deterioration for long periods (Deshwal and Panjagari, 2020). Most used metals for can fabrication are aluminum (Al), coated steels (e.g. chromium-coated tin-free and electrochemically tin-plated steels, shortened as TFS and ETP, respectively), and stainless steels (Debeaufort, 2021). However, depending on the chemical nature of the metal and the canned food, these metals need to be protected with an inner polymer coating or lacquer to avoid corrosion and the release of toxic substances. Until now, bisphenol A (BPA)-based lacquers have been massively used as can coating. BPA lacquers are epoxy resins produced by the reaction between epichlorohydrin with bisphenol A in the presence of sodium hydroxide. The global volume of these epoxy resins for the production of BPA-based lacquers reached ~0.35 million tons in 2021 (ECHEMI, 2021; PlasticsEurope, 2022). The choice of these epoxy resins is based on their excellent anti-corrosion behavior, mechanical robustness, thermal stability, chemical inertness, easy processability, and low price (Pham and Marks, 2005). In addition, they retain their physical and chemical properties for long periods of storage and under harsh conditions. Nevertheless, BPA presents important sustainability and health concerns. On one hand, the BPA synthesis is dependent on fossil resources and consists of the bulk condensation of phenol and acetone catalyzed by ion exchange resins and promoted by mercapto-group containing compounds (Ma et al., 2016; Prokop et al., 2004). On the other hand, the release of BPA molecules from epoxy resins to canned food and their intake has been related to problems during sexual development, metabolic dysfunctions, and neurodevelopmental and immune disorders due to the disruption of the estrogen biochemical pathways (Tassinari et al., 2020). As a consequence, many governments (e.g. Canada, European Union, among others) have limited or banned its use. To avoid these restrictions, many manufacturers are using alternative substances, such as bisphenols F and S, although their innocuousness for human health is also questioned (Fouyet et al., 2021).

The quest of innocuous, sustainable, and economically viable alternatives to BPA-based lacquers is an important objective of the chemical industry. Most of them are based on partial bio-based versions of common can coatings (i.e. oleoresins, phenolics, acrylics, vinyls, and other types of epoxies), although they do not meet all technical requirements and only can be used for specific foodstuffs (Bomgardner, 2013; Simal-Gándara, 1999). In a circular bioeconomy context, fully bio-based polymers are presented as an attractive option, since they can replace petroleum-based plastics as safe and environmentally friendly substitutes. Furthermore, bio-based and biodegradable polymers from renewable resources that are not used for food or animal feed are an interesting alternative for the fabrication of bioplastics in terms of environmental impact, although other uses such as biofuel production or biomedical materials preparation, by conventional or innovative methodologies, can be also considered (Hamzah et al., 2022). This is the case of many food by-products and wastes such as bagasse, husks, peels, etc. generated as residues in food processing (Tsang et al., 2019). In recent years, tomato pomace (the resultant by-product of industrial tomato fruit processing) has been used for the preparation of animal feed, food ingredients, absorbent materials, and biofuels as well as a source of bioactive compounds (Lu et al., 2019). In particular, tomato pomace extracts have found applications in cosmetics (Vasyliev et al., 2022), food packaging (Andres et al., 2017), and anticorrosion uses (Vorobyova and Skiba, 2022). These extracts are rich in polar compounds, while non-polar ones are not frequent. In addition, this by-product has been also upcycled for the production of bio-based polymeric materials (Maraveas, 2020). For instance, pectin (Namir et al., 2015; Zhang et al., 2020) and cellulose (Pirozzi et al., 2022) from tomato pomace have been extracted and used for biodegradable polymer production. The lipid fraction of this by-product (mainly formed by cutin, an aliphatic polyhydroxylated polyester, whose main monomer is the 10,16-dihydroxyhexadecanoic acid, from the peels and unsaturated fatty acids such as oleic and linoleic acids from the seeds) has been also used for the fabrication of functional materials such as films (Benítez et al., 2018; Heredia-Guerrero et al., 2017), coatings (Guzmán-Puyol et al., 2021), composites (Aloui et al., 2019; Heredia-Guerrero et al., 2017), oligomers (Escórcio et al., 2022), etc. In this sense, tomato pomace can be envisaged as an accessible and cost-effective source of fatty acids and hydroxyacids competing with other extractions or synthetic pathways because simple, high-yield and scalable industrial processes such as hydrolysis/neutralization are solely required.

In this work, we report the fabrication of bio-based coatings that can be used as inner protective lacquers of cans. For this, an inexpensive and underutilized agro-food residue, such as the tomato pomace, has been upcycled and its lipid fraction extracted, processed and polymerized on different metal substrates (i.e. Al, TFS, and ETP). The chemical (degree of polymerization), morphological (surface texture), and physical (water-contact angle, surface energy, and mechanical and anti-corrosion properties) features of these coatings were characterized and the role of the metal substrate elucidated. Physical properties were compared with those of common petroleum-based plastics and bio-based polymers used in food packaging as well as resins and lacquers utilized in metal packaging. In a wider perspective, the sustainability of the proposed methodology of fabrication was determined by life cycle analysis (LCA). The evaluation by LCA had multiple objectives: the quantification of the environmental improvements, compared to previous treatments described for the production of bio-based polymers by hydrolysis of tomato pomace (Amato et al., 2021; Benítez et al., 2018), the comparison with the baseline scenario, including the most common ways of tomato residue management as a waste, and the analysis of the environmental burden related to the process stages.

2. Materials and methods

2.1. Materials

Tomato pomace was supplied by "Conservas Martinete S.A." located at Puebla de la Calzada, Badajoz, Spain. It is obtained as the residue of the processing of four-lobulated industrial tomato fruits. NaOH (>99%), HCl (37%), and ethanol (96%) were purchased from Merck and used without additional purifications. Water was Milli-Q (Millipore) grade. Aluminum (Al), chromium-coated tin-free steel (TFS), and electrochemically tin-plated steel (ETP) were kindly provided by Akzo Nobel Coatings S.L, Spain.

2.2. Extraction of the lipid fraction of tomato pomace

The lipid fraction of tomato pomace was isolated following the methodology described elsewhere (Benítez et al., 2018) with some modifications. First, wet by-products after tomato crushing at the factory were sun-dried in situ for 2–3 days and stored in hermetic plastic bags until further drying (4 h later) at 60 °C for 16 h in an oven. Then, the residue was ground with a rotor mill equipped with a stainless steel sieve ring with 0.08 mm trapezoidal perforations. After, 3 g of dried and ground tomato pomace was heated under reflux at 100 °C for 4 h in 75 mL of a 1 M NaOH aqueous solution. The non-hydrolysable residue, obtained after the alkaline treatment, was separated by filtration. The

monomeric mixture was recovered from the hydrolysis filtrate by acidification with a 37% HCl aqueous solution until pH 3. The precipitate was separated by filtration and re-dispersed in water for three times to remove the NaCl residues. The final product, ~32% of the dry tomato pomace, was isolated by filtration and dried at 60 °C for 16 h in an oven.

2.3. Coating preparation

A sprayable paste was generated by blending 1 g of the lipid fraction of tomato pomace with 1 mL of a mixture ethanol:H_2O (3:1, v:v) at 50 °C for 5 min in a hot-plate. Then, such a paste was quickly sprayed by hand using an airbrush (0.5 mm nozzle) on previously cleaned square metal substrates (4.5 × 4.5 cm^2) until a lipid surface concentration of 0.6 mg/cm^2. Air pressure and paste flow were adjusted to obtain a visually continuous and flat layer. The coating was dried at room temperature and the polymerization by melt-polycondensation was conducted at 200 °C at times ranging from 10 to 60 min inside an air-forced oven. Considering the density (~1.1 g/cm^3) of this type of polyesters (Tedeschi et al., 2020), the substrate area and the weight different between coated and non-coated substrates, the thickness was estimated to be 5–6 μm.

A schematic representation of the whole process, comprising the extraction of the lipid fraction and the coating fabrication, is displayed in Fig. 1A.

2.4. Morphological characterization

The morphology of the coatings was observed by Scanning Electron Microscopy (SEM) by using a JEOL JSM-6490LA microscope, operating in high vacuum mode and acceleration voltage of 15 kV. Samples were previously covered with a thin film of gold ~10 nm thickness by using a JEOL ION SPUTTER JFC 1100. The motif's diameter was calculated with ImageJ 1.52a software. Basically, the SEM images were loaded into the software and the motif's diameter was measured using a two-point measuring analysis. One hundred measurements were taken to calculate the diameter distribution.

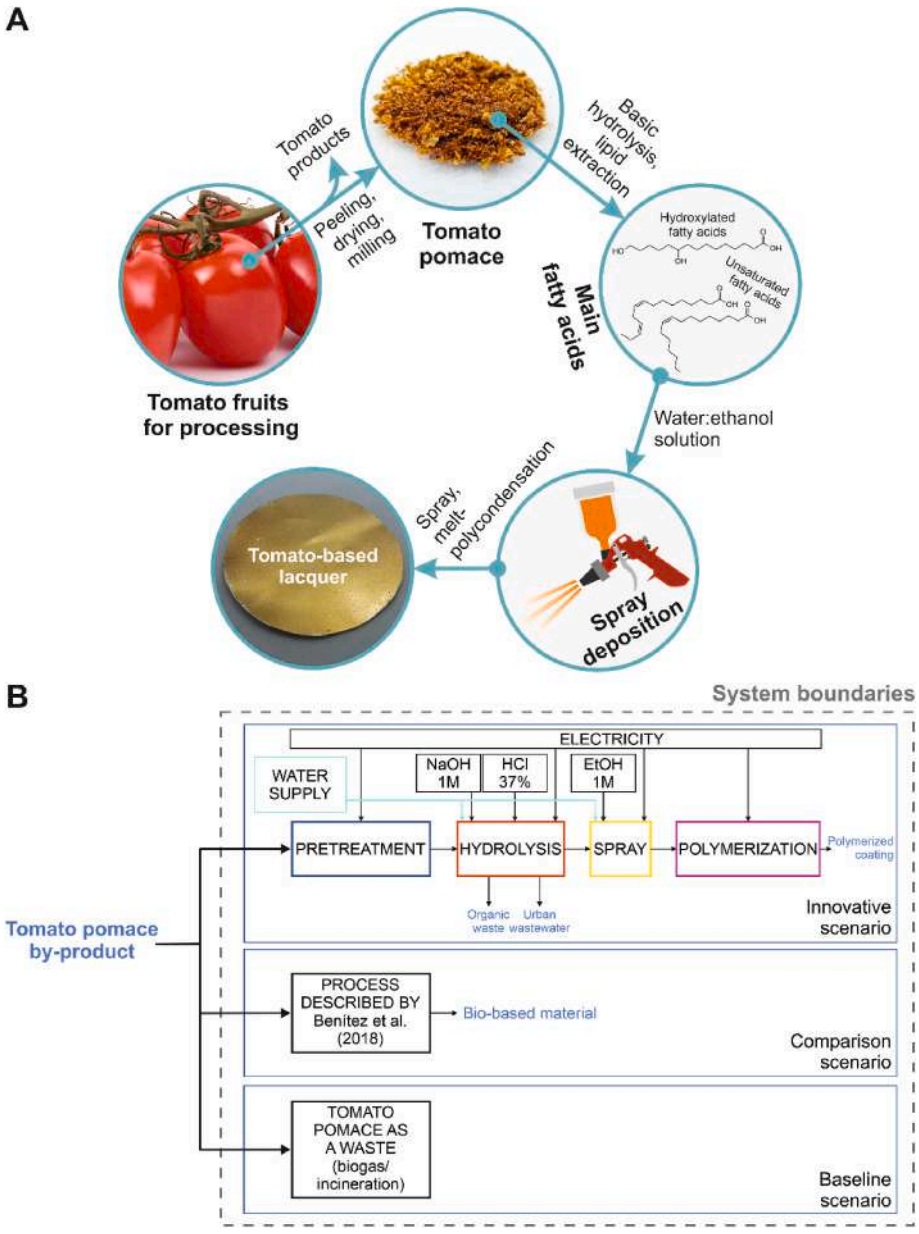

Fig. 1. **A**, schematic representation of the fabrication process of the tomato pomace-based lacquers for metal packaging. First, tomato fruits are processed to prepare different tomato products (e.g. sauces, soups, ketchup, etc.). The resulting by-product, namely tomato pomace, is hydrolyzed in basic media and the corresponding hydroxylated and unsaturated fatty acids from peels and seed, respectively, are extracted. These molecules are solved in a mixture of water and ethanol and sprayed on a metal substrate. Finally, a bio-based polyester is prepared by melt-polycondensation. **B**, system boundaries considered for the LCA.

2.5. Chemical analysis

Coatings were chemically characterized by FT-IR spectroscopy using a specular reflectance accessory (Smart SpeculATR, Thermo Scientific) coupled to a Nicolet iS50 spectrometer and equipped with a DLaTGS detector. The equipment was continuously purged with dry N_2 to reduce the contribution of ambient CO_2 and water. The analysis area was ~3.1 cm^2, which ensured high signal levels and sample representativeness. Fifty scans were accumulated at 4 cm^{-1} resolution and clean metal supports were used as backgrounds. Data acquisition and processing were performed with the OMNIC 9 (Thermo Scientific) software package. Band fitting of C═O components (1800-1650 cm^{-1}) was carried out by using the PeakFit 4.11 software. Wavenumber positions of the different components (i.e. free ester groups, esters interacting by H-bonds, and carboxyl groups) were determined by calculation of the second-order derivative. Deconvolution was performed using Gaussian shape with an amplitude threshold of 3%. A non-linear least-square method was employed to reduce the differences between the calculated spectra and the original one.

2.6. Delamination resistance

The adhesion of the coatings on the three different substrates was determined by scratch tests on a MicroCombi system (Anton Paar), equipped with a spheroconical Rockwell tip (radius = 100 μm). Delamination resistance was measured through scratch tests with increasing load, from 30 to 5000 mN, through a lateral displacement of 2 mm. During the test, lateral force and tip penetration were recorded. After each test, the critical loads for the onset of visible mechanisms of damage were detected with the built-in microscope. Three different measurements were conducted for each sample.

2.7. Wettability

The wettability of the coatings was determined by using a contact angle DataPhysics OCA 200 goniometer and measuring the corresponding static water contact angles (W-CA) at room conditions. Milli-Q water droplets of 5 μL volume were deposited on 10 different places of each surface and their lateral images captured. After 2 min (to reach the equilibrium), the water contact angles were determined by SCA 20 software. The surface free energy of the biocomposites was estimated by calculations from the Owens, Wendt, Rabel & Kälble (OWRK) method (Owens and Wendt, 1969) applied at two solvents (water and diiomethane, Table S1) (Ström et al., 1987), as reported elsewhere (Tedeschi et al., 2018).

2.8. Electrochemical characterization

Electrochemical impedance spectroscopy (EIS) was employed to evaluate the anticorrosion performance of the coatings by using a homemade electrochemical cell in a two-electrode configuration, in which the coated metal substrate was the working electrode and a Pt mesh served as a counter electrode. A cylindrical glass tube with an O-ring seal was clamped to the coated samples under test. A sample area of 1 cm^2 was exposed to an aqueous solution of 1 wt% NaCl. The choice of this corrosive medium is based on the corrosive behaviour of chloride-containing salts and on the fact that NaCl is widely used as an additive in canned foods (Morselli et al., 2021; Upadhyay and Battocchi, 2016). A Solartron 1260 frequency response analyzer was used for the electrochemical impedance measurements in the frequency range from 5×10^{-3} to 10^6 Hz (8 point per decade), using an ac amplitude of 50 mV at open circuit voltage. The impedance spectra were acquired in time intervals of 2–5 h during an overall stability test up to 170 h. For comparison purposes, the unprotected metal substrates were also studied under identical experimental conditions. The impedance spectra were analyzed by equivalent circuit models with ZView software (Scribner Associates) to determine the resistance and capacitance of the different processes occurring at the metal/coating interface.

2.9. Life cycle analysis (LCA)

A Life Cycle Assessment methodology was applied in agreement with the LCA ISO standard 14040 and 14044:2006 ("ISO 14044:2006 Environmental management – Life cycle assessment – Requirements and guidelines," 2006, *UNI EN ISO 14040: 2006. Environmental management – life cycle assessment – principles and framework.*, 2006). The software used for data collection was Thinkstep Gabi 9.2.1.68, combined with the Database for Life Cycle Engineering. The method selected for the analysis, which included the classification and characterization steps, was Environmental Footprint 3.0, including all environmental categories, recommended models at midpoint, together with their indicators, units and sources (Commission, 2012; Zampori and Pant, 2019). The functional unit chosen for the process analysis was 4 kg of wet tomato pomace that resulted in 1 kg of dried tomato pomace, after drying. The system boundaries considered for the present study have been summarized in Fig. 1B.

Some assumptions were taken for the analysis. The electricity consumption was halved compared to the lab scale machines demand, on average more energy-intensive that industrial ones. This assumption allowed to include the possible reduction of environmental impact associated with the process scale-up (from TRL4), as discussed elsewhere (van der Hulst et al., 2020). Thus, in a context of circular economy, the electricity production by photovoltaic resources can be hypothesized. This assumption was considered realistic in view of the common installation of photovoltaic systems on industrial buildings and the high solar radiation availability in the areas of tomato cultivation and processing. Regarding the spray deposition step, the recovery of 50% of ethanol was hypothesized (after the vapor condensation). Material and energy balances related to this innovative scenario are reported in Table S2, following the experimental results. The benefit of the resulting resin was quantified as the credit for the avoided primary production of a traditional epoxy resin. Regarding the comparison scenario, the environmental impacts were extracted by the results described by Amato et al. (2021). For the baseline scenario, the use of tomato pomace for biogas production was considered (Boccia et al., 2019). As an alternative to the biogas production, the effect of the CO_2 emissions from the residue incineration (without energy recovery) was assessed since it is a common practice in agriculture (Nguyen et al., 2019). Additional alternatives such as the disposal in landfilling sites (Cuccolini et al., 2013; Grassino et al., 2016) and the production of animal feed, which represent extra-costs and an environmental concern for the tomato processing industry (Silva et al., 2019), have been excluded, as previously highlighted in the GRASCIARI RIUNITI Project (Amato et al., 2021).

3. Results and discussion

3.1. Chemical characterization of the coatings

The melt-polycondensation reaction between the fatty acids (mainly, 10,16-dihydroxypalmitic acid, see Table S3) of the lipid fraction of the tomato processing by-products was characterized by specular reflectance infrared spectroscopy, Fig. 2. This technique is indicated for the analysis of coatings due to the large areas that can be tested and the adequate penetration depth of the beam. Moreover, the signal is quantitative when expressed as log *(1/R)*, i.e. the logarithm of the inverse of the relative reflectance (Benítez et al., 2020). The reaction was monitored each 10 min up to a maximum of 60 min, maintaining a constant temperature of 200 °C. Fig. 2A shows some representative spectra corresponding to the coatings on Al, ETP, and TFS at 10, 30, and 60 min, respectively. As a reference, the IR spectrum of the lipid fraction extracted from tomato pomace is included. Main bands of the lipid

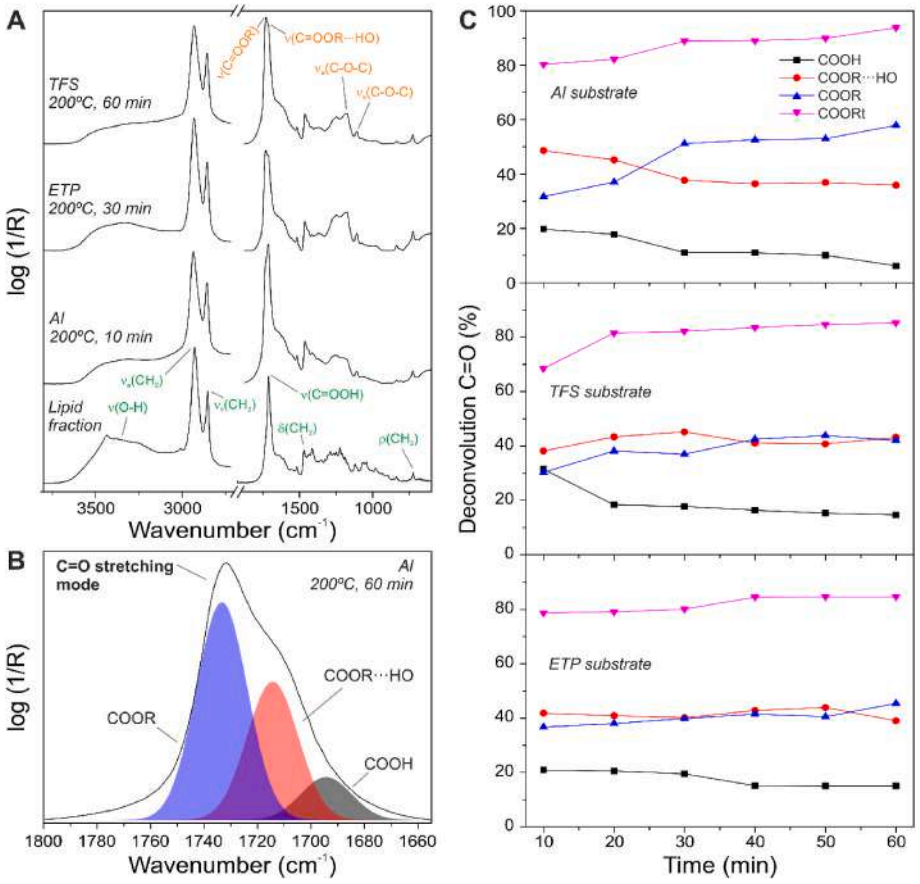

Fig. 2. A, specular infrared spectra of the coatings prepared at 200 °C on Al, ETP, and TFS substrates for 10, 30, and 60 min, respectively. As a reference, the IR spectrum of the lipid fraction from tomato pomace is included. Main assignations for the lipid fraction (green) and polyester (orange) are included. **B**, example of band fitting into three contributions (COOH in grey, COOR···HO in red, and COOR in blue) of the C═O stretching mode of the coating prepared at 200 °C on Al for 60 min. **C**, percentages of the COOH, COOR···HO, and COOR contributions as well as the one of total ester (COORt) of the C═O stretching mode of the coatings prepared at 200 °C on the different metal substrates as a function of the polymerization time.

fraction were assigned as follows: O-H stretching mode at 3327 cm^{-1}, asymmetric and symmetric CH_2 stretching modes at 2922 and 2850 cm^{-1}, respectively, C═O stretching mode of carboxyl groups at 1703 cm^{-1}, CH_2 deformation mode at 1464 cm^{-1}, and CH_2 rocking mode at 721 cm^{-1} (Heredia-Guerrero et al., 2019). In addition, several bands of medium and low intensity between 1350 and 800 cm^{-1} were associated with the "progression bands", a set of twisting and wagging vibrations of methylene groups caused by the zig-zag crystalline packing of aliphatic chains (Bellamy, 1980; Snyder and Schachtschneider, 1963). Some changes were observed in the spectra of bio-based coatings: a decrease of the O-H stretching and deformation (1050-1100 cm^{-1}) modes of primary and secondary hydroxyls, a shift of the C═O stretching mode at ~1728 and ~1713 cm^{-1} (attributed to free and H-bond interacting ester groups, respectively), the apparition of new bands at 1249 and 1176 cm^{-1} (that are attributed to C-O-C stretching modes of ester groups), and the disappearance of the progression bands. This is indicative of a consumption of hydroxyl and carboxyl groups to result in ester bonds in an amorphous polymer matrix. In addition, it is expected the formation of oxidized species from unsaturated fatty acids in presence of oxygen and at this high temperature of polymerization (200 °C), although they are not detected by specular infrared spectroscopy.

To determine the degree of esterification, the spectral region between 1800 and 1650 cm^{-1}, that is corresponded with the C═O stretching mode of COOR and COOH groups, was deconvoluted considering three contributions: carboxyl, free ester, and H-bond interacting ester groups. As a representative example, the fitting for the coating on aluminum prepared at 200 °C for 60 min is displayed in Fig. 2B. Fig. 2C reports the percentages of the above mentioned contributions plus the COORt (i.e. total esters or the sum of the % of free and H-bond interacting ester groups) calculated from the infrared spectra of the three coating series on Al, TFS and ETP substrates. In general, the percentage of carboxylic acids decreased with heating time, while total esters increased, indicating a consumption of COOH groups to form esters. For TFS and ETP, the percentages of free and H-bond interacting esters were very similar (~40%), whereas for Al COOR and COOR···HO inversed the percentages (~30 and ~50%) between 10 and 30 min of reaction. In addition, the profile of %COORt with the time depended on the metal substrate used. In the case of Al, the percentage of total ester increased progressively from ~80% at 10 min to ~94% at 60 min. For TFS, the %COORt increased from ~69% at 10 min to ~82% at 20 min and, then, slowly reached ~85% at 60 min. Finally, for the coatings on ETP, the %COORt was ~80% in the 10–30 min interval and then increased to ~85% for 40–60 min. The higher %COORt in Al substrates can be related to a better removal of water molecules during the polycondensation in comparison with ETP and TFS. In fact, water presents a high affinity for the Al_xO_y passivation layer on the Al substrate, being adsorbed by O-vacancy defects through a dissociative mechanism that induces the formation of hydroxyl groups (Deng et al., 2008). Interestingly, the ester conversion is higher than the one observed for polyaleuritate (viz. the polyester derived from the polycondensation of aleuritic or 9,10,16-trihydroxypalmitic acid) coatings prepared on the same substrates and similar conditions (Benítez et al., 2020). In these cases, the highest percentages of total ester were close to 60–70%, depending on the metal substrate used. The better polymerization of the lipid fraction of the tomato pomace can be attributable to a more effective water removal due to the fluidity of the system caused by the lubricity of unsaturated fatty acids and a higher hydrophobicity as a consequence of a lower number of hydroxyl groups per molecule when compared to aleuritic acid.

The coatings on the metal substrates were examined by SEM, Fig. 3. In all cases, a smooth coating surface with randomly distributed micrometric particles were observed. Particle size distribution was more homogenous on Al and TFS coatings, while on ETP the particles agglomerated in some regions, Fig. 3A–C. In addition, the coating on

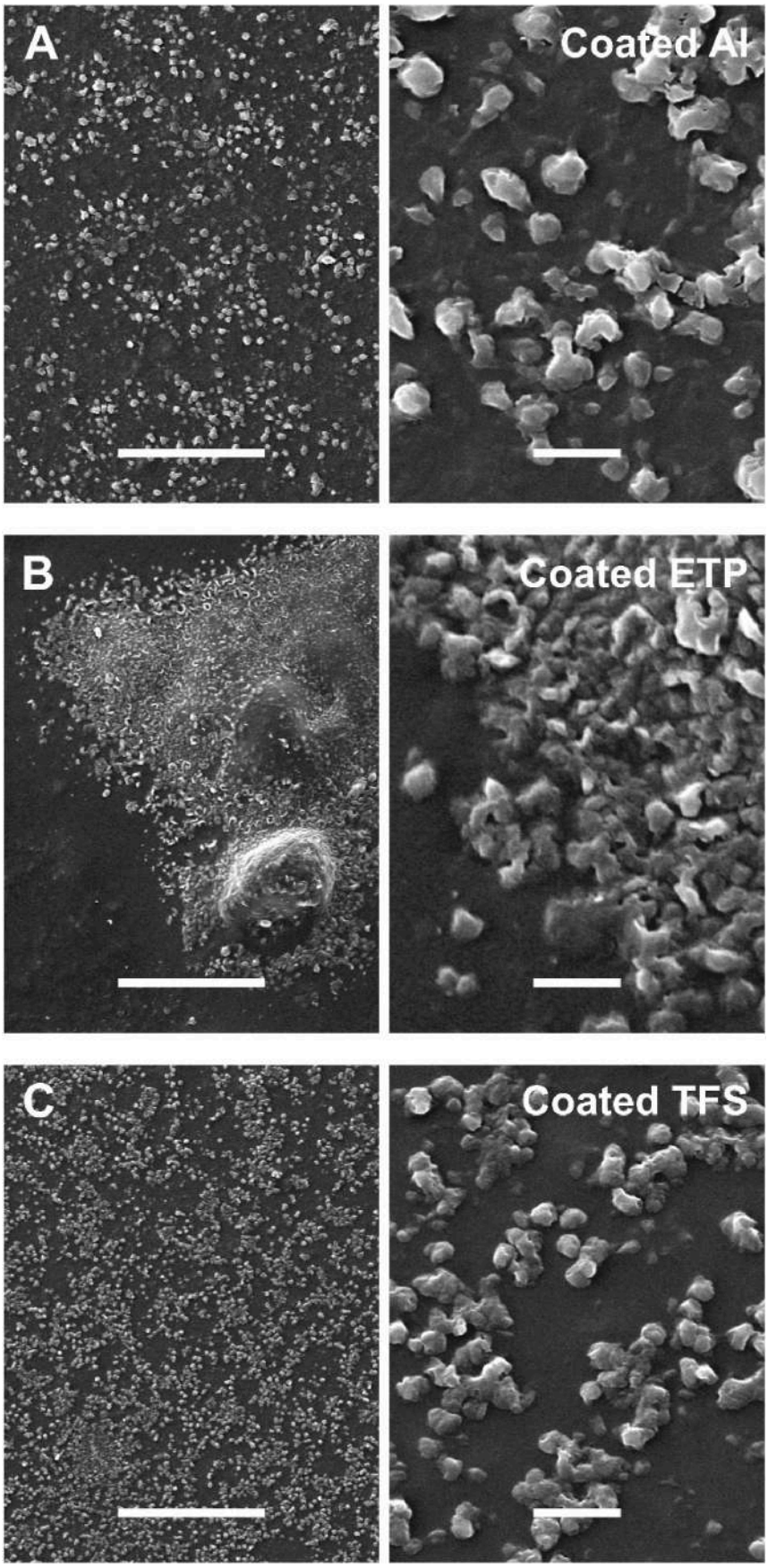

Fig. 3. **A**, **B**, and **C**, lower (left) and higher (right) magnifications of SEM top-view images of the tomato pomace-based coatings on Al, ETP, and TFS, respectively. Scales bars: left – 50 μm, right – 5 μm.

ETP also showed globules of a few tens of microns, Fig. 3B at left. The diameter of the microparticles was evaluated and showed a narrow diameter distribution with averages of (0.9 ± 0.3) and (1.0 ± 0.3) μm for ETP and TFS, respectively. Those on Al exhibited a broader distribution of values whose average was (1.3 ± 0.6) μm.

The surface of analogous pure aleuritate coatings on these supports showed a more continuous and crystalline texture (Benítez et al., 2020), while in the coatings from the lipid fraction of tomato pomace, the amorphous underlying phase is better observed. This can be caused by the heterogeneous composition of the tomato pomace extract that led to structurally unmatched mixed structures, forming a disordered polyester matrix. In addition, and if compared to aleuritic acid, the esterification of the tomato pomace extract is faster. The reason for such a difference can be due to the reaction displacement caused by a better removal of water molecules from a more hydrophobic and fluid medium, as considered above for the infrared analysis. These same factors facilitate the segregation of the more highly hydroxylated components of the monomeric mixture and their slower esterification on top of the amorphous matrix, giving rise to the observed particles in the SEM images. Such a diffusion process is hindered by the faster development of the amorphous phase and justify the lower concentration of particles on substrates with the higher efficiency towards the esterification (Al > TFS > ETP).

3.2. Physical characterization of the coatings

The wettability and the surface energy of the coatings were evaluated by determining the water-contact angle (W-CA), Fig. 4. Fig. 4A at left shows the W-CA values of the coatings prepared at 200 °C for 60 min on the different metal substrates: ~95° for Al, ~91° for ETP, and ~88° for TFS. All these values are typical of hydrophobic materials. The differences among them, considering a similar surface morphology, can be ascribed to the degree of polymerization. A higher polycondensation rate is indicative of a lower presence of polar groups such as carboxyls and hydroxyls that decrease the hydrophobicity. In fact, a linear dependence with a good adjustment ($R^2 = 0.9828$) was observed when the W-CA values are plotted as a function of the %COORt, Fig. 4A at right. Such an argument is completed with the effect of the lower concentration of polyhydroxyester particles on the surface of coatings formed at higher rate. These W-CAs were compared with those reported in the literature for several petroleum-based plastics such as polyethylene terephthalate or PET, high- and low-density polyethylene or HDPE and LDPE, respectively, and oriented polypropylene or OPP (Mirabedini et al., 2007; Westerdahl et al., 1974) and biodegradable polyesters, for example polylactide or PLA, poly-3-hydroxybutyrate or P3HB, and polycaprolactone or PCL typically used in food packaging (Heredia-Guerrero et al., 2019; Morselli et al., 2021) as well as other lacquers and resins (e.g. acrylic, polyester, and epoxy resins) employed in metal packaging (Pajarito et al., 2018; Pilch-Pitera, 2014). All coatings fabricated from the tomato pomace extract showed W-CAs higher than commercial lacquers and resins. The coatings on TFS and ETP presented values close to P3HB, while the one on Al exhibited a WCA similar to polypropylene, both types of polyethylene, and polycaprolactone.

The surface energy of the bio-based coatings and its dispersive and polar contributions were also determined, Fig. 4C. The surface energy of the coating on the Al substrate was ~34 mN/m, while for those on TFS and ETP the value increased to ~44 mN/m, indicating a higher wettability. The dispersive component was almost the totality of the surface energy, with negligible contribution of the polar component, a behavior typical of aliphatic polymers. Similarly to the water-contact angles, these surfaces energies were compared with those of other petroleum-based and bio-based polymers (e.g. PLA, OPP, LDPE, HDPE, PCL, P3HB, and PET) as well as lacquers and resins (e.g. acrylic and aromatic polyester resins and bisphenol-A diglycidyl ether or BADGE). The coatings on TFS and ETP were located between PET and BADGE in the region with higher values. On the other hand, the coating on Al was in the middle with values similar to the aromatic polyester and acrylic resins.

The resistance of the coatings fabricated at 200 °C during 60 min to deformation or removal by accidental localized contact was evaluated by scratch tests, Fig. 5. Different damage mechanisms in ETP and TFS samples as compared with Al were observed, Fig. 5A and B. The formers showed chipping of the coating, starting from radial cracks, while the latter displayed only substrate exposition from plunging. For this change of mechanism, ETP and TFS samples yielded similar critical loads (1078 ± 31 mN and 852 ± 206 mN, respectively), while the value on Al was significantly higher, 1739 ± 198 mN. This behavior can be related with

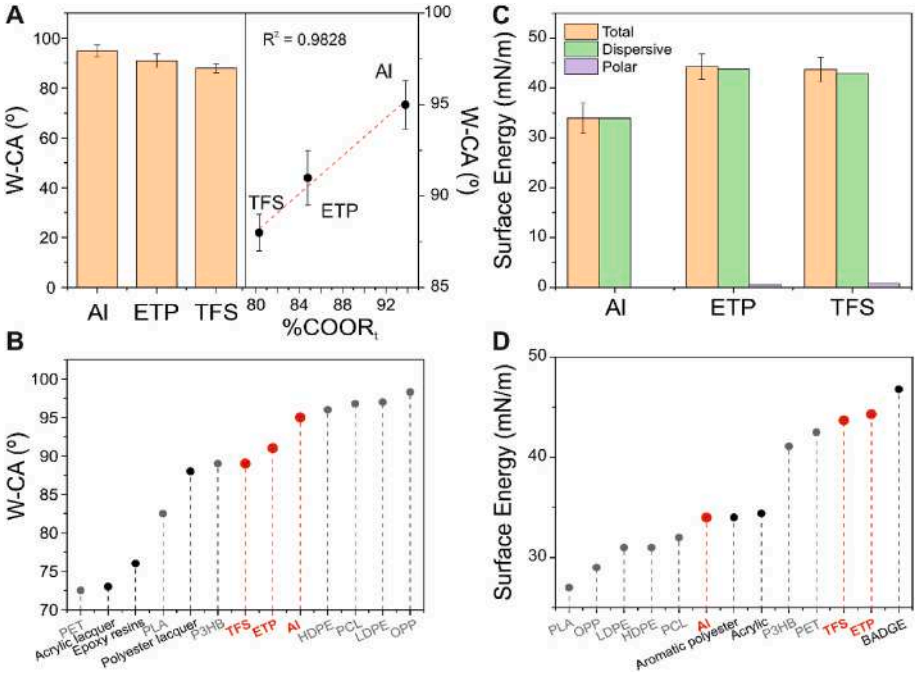

Fig. 4. **A**, left, water-contact angles of the lacquers prepared on the metal substrates at 200 °C for 60 min and, right, relationship between the water-contact angle and the total ester percentage. **B**, comparison of the water contact angles of the lacquers prepared on the metal substrates at 200 °C for 60 min with those of common polymers (grey) and lacquers (black) used in food packaging. **C**, surface energy values, including the dispersive and polar contributions of the lacquers, prepared on the metal substrates at 200 °C for 60 min. **D**, comparison of the surface energies of the lacquers prepared on the metal substrates at 200 °C for 60 min with those of common polymers (grey) and lacquers (black) used in food packaging.

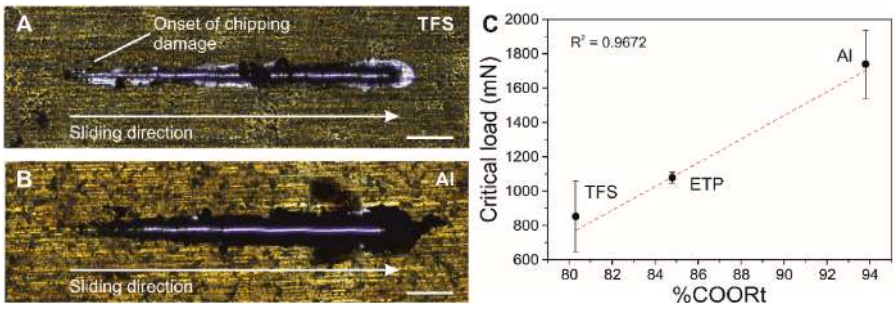

Fig. 5. Scratch test images corresponding to the coatings on, **A**, TFS and, **B**, Al substrates. **C**, linear relationship between the critical load and the percentage of total esters.

the degree of polymerization that determines the mechanical properties of a polymer, Fig. 5C. In fact, there is a linear correspondence (with a $R^2 = 0.9672$) between the critical load of the coatings and their %COORt.

EIS measurements provide information on the protective properties of the coating and the electrochemical processes occurring at the coating/metal interface (Amirudin and Thieny, 1995; Mansfeld, 1995). Examples of Nyquist plots for uncoated and coated Al substrates at different immersion times in NaCl are shown in Fig. 6A and B, respectively. The different contributions of the impedance data were analyzed by equivalent circuit models reported in the literature for uncoated and polymer coated metals, as shown in Fig. 6C and D, respectively. A dry polymer coating behaves like a dielectric layer before immersion. However, they are not usually perfect barriers against a corrosive medium due to water uptake or penetration. In general, the water permeability decreases for those organic coatings with higher density and cross-linked structures due to limited paths for diffusion. In these equivalent circuits, R_s represents the solution resistance and R_c corresponds to the coating and pore resistance associated with the formation of conducting paths across the coating. R_{ct} is the charge polarization resistance at the metal/coating interface at which corrosion occurs and Q_{dl} is the corresponding double layer capacitance. Since the different processes in the Nyquist plots are depressed semicircles, the ideal capacitances are replaced by constant phase elements Q that account for non-uniform and geometrical effects of the coating and substrate such as time constant variations, mass transfer processes, and other deviations. Thus, the real capacitance C is determined using the following equation (Irvine et al., 1990), Equation (1):

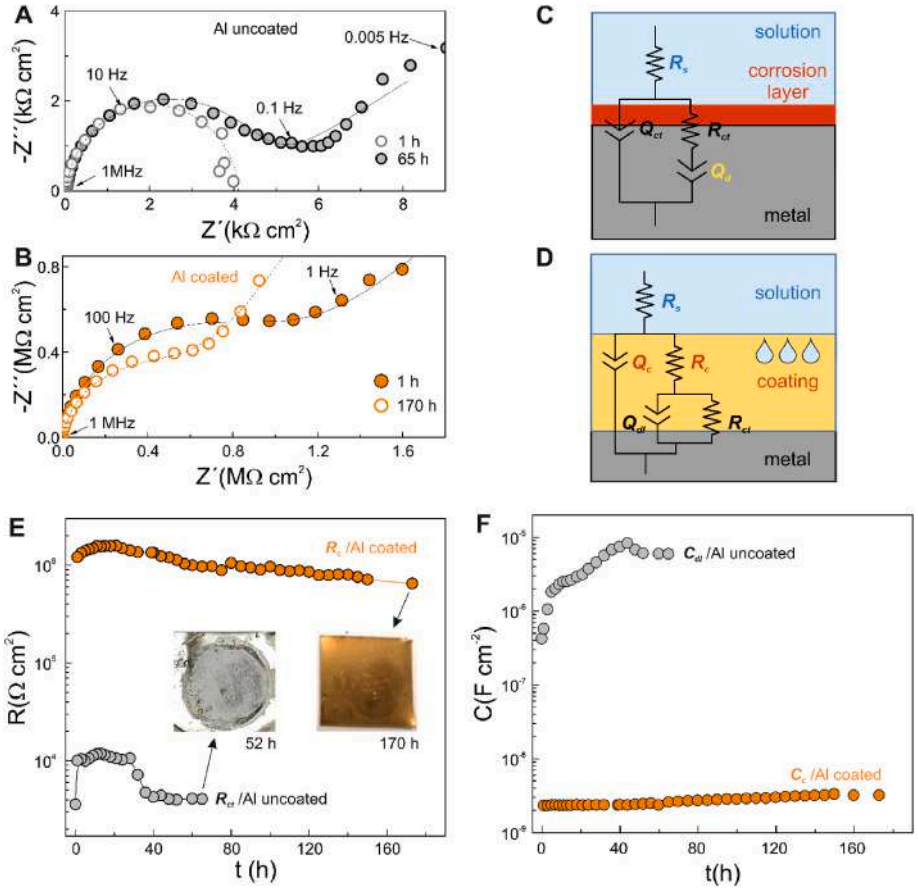

Fig. 6. Nyquist plots at different immersion times for, **A**, uncoated and, **B**, coated Al substrates. Equivalent circuit models used for the analysis of EIS data of, **C**, uncoated and, **D**, coated substrates. **E**, variation of the coating resistance R_c and charge transfer resistance R_{ct} for the coated and uncoated Al substrates, respectively. **F**, variation of the coating capacitance C_c and double layer capacitance C_{dl} for the coated and uncoated Al substrates, respectively.

$$C = \frac{(RQ_0)^{1/n}}{R} \quad (1)$$

where Q_o is the pseudocapacitance and n is the corresponding exponential coefficient to consider the non-ideal capacitive behavior.

The Nyquist plots for the uncoated Al substrate at the beginning of the durability test showed a semicircle assigned to a charge transfer reaction at the metal/solution interface, Fig. 6A. A second contribution appeared at the low frequency range after several hours of immersion into the NaCl solution due to the formation and ion migration through an oxide layer, which could be simulated by a Warbung diffusion phenomena or alternatively by a constant phase element Q_d (Caldona et al., 2020; El hadad et al., 2020). Such a corrosion layer became thicker over immersion time, initially resulting in an increase of both the charge transfer resistance R_{ct} and double layer capacitance C_{dl} at the electrolyte/metal interface, Fig. 6E and F. However, this corrosion layer is not stable after prolonged immersion times, resulting in delamination with a remarkable reduction of R_{ct}, inset in Fig. 6E.

The Nyquist plots of Al coated substrate displayed a semicircle at high frequency, assigned to the coating resistance, and a loop a low frequency related to electrode processes at the metal interface. The properties of the charge transfer processes were not correctly determined by using the equivalent circuit of Fig. 6D because an incomplete semicircle was observed at low frequency, which resulted in R_{ct} values higher than 10^{15} Ωcm^2, thus this component approached to infinite impedance. This fact allowed to simplify the equivalent circuit by removal the R_{ct} element in Fig. 6D. As observed in Fig. 6E, the coating resistance decreased slightly over time from ~1 MΩcm^2 at the initial state of the durability test to 0.7 MΩcm^2 after 170 h. Such a behavior was associated with water penetration into the coating, which was accompanied by an increase of the coating capacitance from 2.3 to 3.2 nF cm^{-2}, Fig. 6F (Amirudin and Thieny, 1995; Mansfeld, 1995). However, it is worth noting that the coating structure remained stable over time without the presence of delamination or pilling corrosion, as shown in the inset of Fig. 6E.

In the case of the unprotected TFS substrates, the charge transfer process increased rapidly after only several hours of immersion due to the corrosion products deposited on the metal surface, Fig. S1. In addition, the electrolyte resistance R_s decreased from 83 to 20 Ωcm^2 after 24 h of immersion due to the presence of released ions into the electrolyte solution, which are clearly visible during the stability test, inset of Fig. S1C. The coated TFS substrate exhibited two electrochemical processes in the Nyquist plots and the data were adequately fitted by using the equivalent circuit of Fig. 6D. The coating resistance decreased from 0.8 to 0.7 MΩcm^2 after 70 h of immersion due to water uptake as previously commented, Fig. S1C. Interestingly, the parameters associated with the corrosion of the metal substrate and the electrochemical double layer (R_{ct} and C_{dl}) remained unchanged over time, indicating that during the immersion tests, the coated TFS metallic surface is stable, inset of Fig. S1C. The values of coating capacitance for both Al and TFS are comparable, about 2.4 and 2.7 nC cm^{-2}, suggesting that both protective layers have similar thickness, regardless of the characteristics of the metal substrate.

Finally, the coatings on ETP substrate suffered a rapid decrease of R_c just after immersion, which is possibly associated with an inhomogeneous thickness of the coating, as observed by SEM analysis. In fact, the regions where the coating is thinnest can quickly allow the corrosion process.

In general, the values of coating resistance on Al and TFS are higher than those reported for related organic coatings such as 10^4 Ω cm^2 for chitosan (Bahari et al., 2020), $1.7{\cdot}10^5$ Ω cm^2 for of epoxy coatings containing encapsulated crude vegetal extracts of *Azadirachta indica* (Neem) leaves (Ulaeto et al., 2023) and, $4.92{\cdot}10^5$ Ω cm^2 for a cycloaliphatic epoxide-based UV lacquer (Fragni et al., 2006), to mention a few. However, they are lower than those found for ZnO-modified coatings, for example $2{\cdot}10^8$ Ω cm^2 for a zinc polyaleuritate ionomer coatings (Morselli et al., 2021) and $8{\cdot}10^8$ Ω cm^2 for a bio-based PUA with ZnO coatings (Ariffin et al., 2020).

3.3. Life Cycle Analysis of the coating fabrication process

The results of LCA (classification and characterization) reported in Fig. 7 are key to appreciate the sustainability improvements of the use of tomato pomace for the fabrication of coatings in comparison to the fabrication of bioplastics by the current technology (comparable scenario) and the simple incineration or biogas generation (baseline scenario). It is evident that the technical enhancement of the process was translated into an environmental gain, as highlighted by the comparison between this innovative process and the comparable scenario described by Benítez et al. (2018). The reduction of environmental burden is observed in most of categories and averages ~60%. The advantage of the innovative scenario is explained by the combination of a new process design (with a simpler setup and lower energy and raw materials consumptions), the production of a bio-based lacquer as an alternative to the most common epoxy resin (as represented by the grey environmental credit) and the use of photovoltaic energy. The reduction of organic solvent consumption and the possibility of ethanol recirculation have played an essential role on the sustainability of the innovative process. The benefits of the tomato pomace-based lacquer production are clear in many categories, particularly in the categories connected to the human health (Fig. 7N and O). The contradictory results showed in Fig. 7G and J are due to the effect of photovoltaic panel manufacturing (used for energy supply). Nevertheless, they do not afflict the whole result of the analysis. The environmental gain of the innovative scenario, compared to the baseline one, is less positive in several categories due to the advantage of energy production from biogas. This issue is evident for the climate change category (Fig. 7B), but it should be discussed with a critical thinking for a double reason: first, the use of tomato pomace for biogas production causes the loss of important components still contained in the food waste and, second, not all facilities are equipped by a system for biogas production. When the impact on climate change was reassessed considering the incineration of tomato residue (common practice in agriculture), the result changed drastically. As reported in Fig. 7B, the innovative option allows an environmental benefit ~55%, compared to the impact resulting from the traditional incineration of agriculture residues (1.2 kg CO_2 eq. of innovative scenario vs. 2.8 kg CO2 eq. of incineration).

After this overview of the available scenarios for tomato pomace management, Fig. 8 shows in detail the environmental impact of the innovative process (as the average result of all considered categories). The lipid fraction extraction through the hydrolysis step is identified by far as the driving stage (around 90% of the whole environmental load, Fig. 8A). The explanation of this result is showed in Fig. 8B that focuses on the contribution on each impact category of the parameters involved in the extraction process by hydrolysis. In most cases, the higher impact is due to both sodium hydroxide and hydrochloric acid use and consumption, with a minor contribution of electricity demand and waste flows management. The negative value represented in the water scarcity category is connected to the possibility of water recovery after the discharge and the treatment phases.

4. Conclusions

A by-product such as the pomace resulting from the tomato fruit processing has been used as a renewable raw material in a context of circular bioeconomy. In this sense, safe bio-based lacquers have been fabricated and presented as good alternatives to current BPA-based technologies. For this, the lipid fraction of tomato pomace was extracted by basic hydrolysis and the resulting unsaturated and polydydroxylated fatty acids were sprayed on typical metal food substrates (Al, ETS, and TFS) and polymerized by self melt-polycondensation with no catalysts. The coating on the Al substrate showed the highest rate of

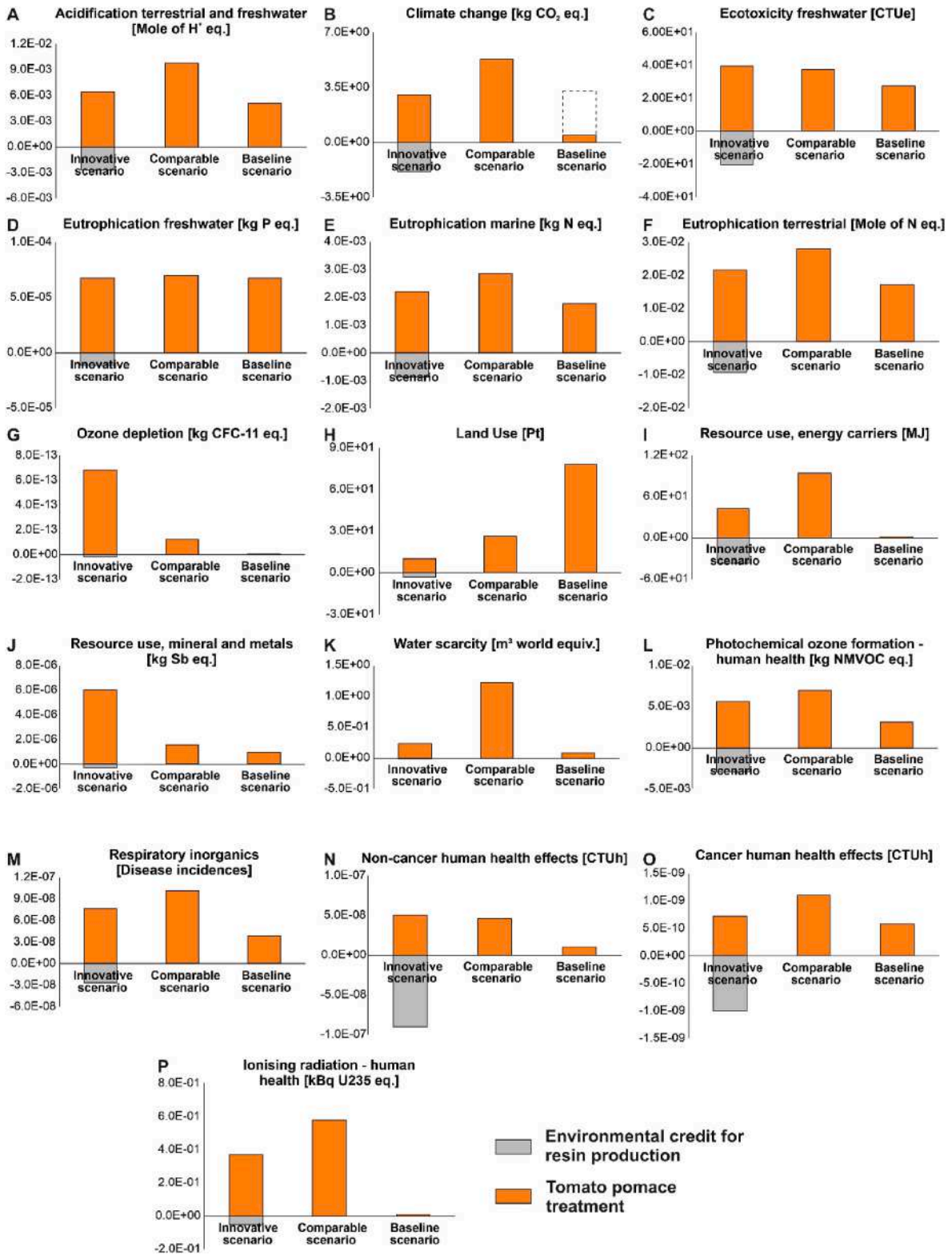

Fig. 7. Results of classification and characterization steps of LCA. Comparison among innovative treatment, comparable scenario described by Benítez et al. (2018) and the baseline scenario with tomato pomace use for biogas production (functional unit 4 kg of wet tomato pomace).

polymerization, most likely due to a better removal of water molecules during the reaction. Hydrophobicity and scratch resistance of coatings depended on the metal substrate used and were better as the degree of polymerization was higher. The studies on the anticorrosion performance revealed that the coatings on Al, and to a lesser extent on TFS, offered an adequate protection against corrosion with coating resistance values close to 10^6 Ω cm^2. The LCA study determined an important gain in terms of sustainability when the production of these bio-based coatings was compared with those of the BPA-based lacquers. Once the potentials of this approach have been presented, further studies are necessary to assert the innocuousness of these coatings related to the migration of potentially toxic substances generated along the coating

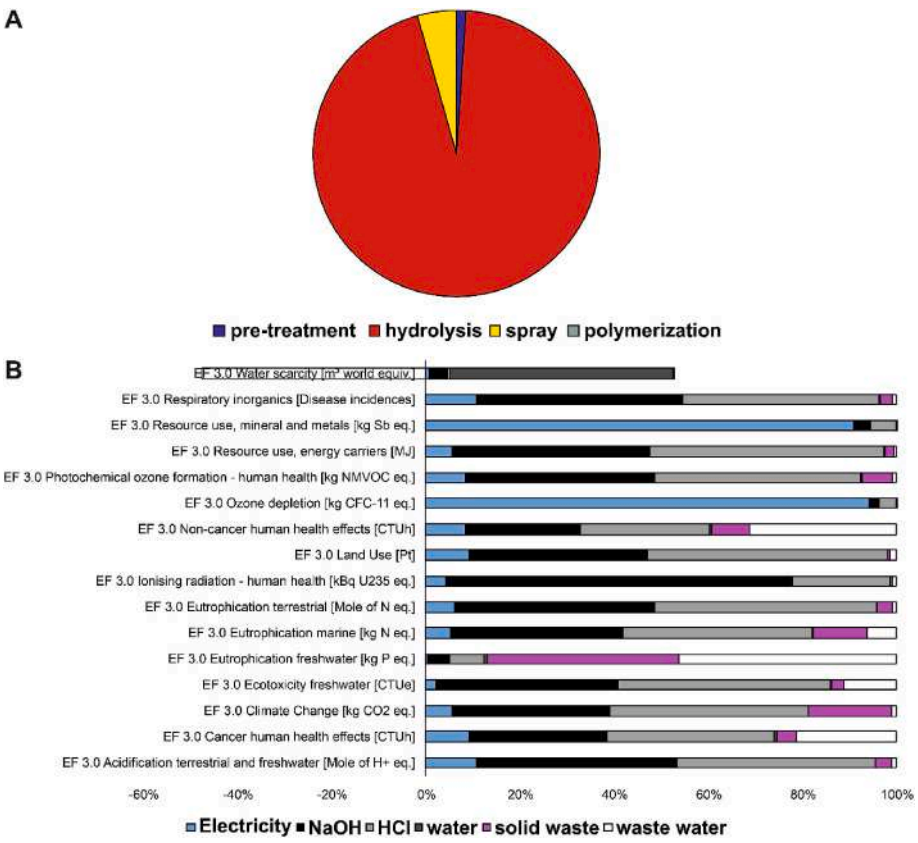

Fig. 8. Environmental sustainability analysis of the: **A**, the different steps of the innovative process and, **B**, the contributions of each parameter in the lipid extraction process through the hydrolysis step in the impact categories. The results of classification and characterization steps of LCA are based on a definition of functional unit of 4 kg of wet tomato pomace.

formation.

CRediT authorship contribution statement

José J. Benítez: Conceptualization, Data curation, Formal analysis, Investigation, Methodology, Supervision, Writing – original draft, Writing – review & editing. **María C. Ramírez-Pozo:** Investigation. **María M. Durán-Barrantes:** Investigation, Supervision. **Antonio Heredia:** Conceptualization, Funding acquisition. **Giacomo Tedeschi:** Data curation, Investigation. **Luca Ceseracciu:** Data curation, Investigation, Writing – original draft. **Susana Guzman-Puyol:** Data curation, Investigation, Writing – original draft. **David Marrero-López:** Data curation, Investigation, Writing – original draft, Writing – review & editing. **Alessandro Becci:** Investigation. **Alessia Amato:** Data curation, Investigation, Writing – original draft, Writing – review & editing. **José A. Heredia-Guerrero:** Conceptualization, Data curation, Formal analysis, Funding acquisition, Investigation, Methodology, Supervision, Writing – original draft, Writing – review & editing.

Declaration of competing interest

The authors declare that they have no known competing financial interests or personal relationships that could have appeared to influence the work reported in this paper.

Data availability

Data will be made available on request.

Acknowledgements

J.A.H.-G. acknowledges the support by the Spanish "Ministerio de Ciencia, Innovación y Universidades" projects RTI2018-096896-J-I00/AEI/10.13039/501100011033 (cofinanced by the European Regional Development Fund, ERDF) and RYC2018-025079-I/AEI/10.13039/501100011033 (cofinanced by the European Social Fund, ESF) as well as by the PIE project 202040E003 funded by CSIC. S.G-P thanks the "Consejería de Transformación Económica, Industria, Conocimiento y Universidades" from Junta de Andalucía for a postdoctoral contract (POSTDOC_21_00008). This works has been also supported by the project UMA20-FEDERJA-067 from "Consejería de Economía y Conocimiento", "Junta de Andalucía", Spain, and the European funds for the Regional development FEASR-PSR MARCHE 2014–2020 within the project GRASCIARI RIUNITI.

Appendix A. Supplementary data

Supplementary data to this article can be found online at https://doi.org/10.1016/j.jclepro.2022.135836.

References

Aloui, H., Baraket, K., Sendon, R., Silva, A.S., Khwaldia, K., 2019. Development and characterization of novel composite glycerol-plasticized films based on sodium caseinate and lipid fraction of tomato pomace by-product. Int. J. Biol. Macromol. 139, 128–138. https://doi.org/10.1016/j.ijbiomac.2019.07.156.

Amato, A., Mastrovito, M., Becci, A., Beolchini, F., 2021. Environmental sustainability analysis of case studies of agriculture residue exploitation. Sustain. Times 13. https://doi.org/10.3390/su13073990.

Amirudin, A., Thieny, D., 1995. Application of electrochemical impedance spectroscopy to study the degradation of polymer-coated metals. Prog. Org. Coating 26, 1–28. https://doi.org/10.1016/0300-9440(95)00581-1.

Andres, A.I., Petron, M.J., Delgado-Adamez, J., Lopez, M., Timon, M., 2017. Effect of tomato pomace extracts on the shelf-life of modified atmosphere-packaged lamb meat. J. Food Process. Preserv. 41, e13018 https://doi.org/10.1111/jfpp.13018.
Ariffin, M.M., Aung, M.M., Abdullah, L.C., Salleh, M.Z., 2020. Assessment of corrosion protection and performance of bio-based polyurethane acrylate incorporated with nano zinc oxide coating. Polym. Test. 87, 106526 https://doi.org/10.1016/j.polymertesting.2020.106526.
Bahari, H.S., Ye, F., Carrillo, E.A.T., Leliopoulos, C., Savaloni, H., Dutta, J., 2020. Chitosan nanocomposite coatings with enhanced corrosion inhibition effects for copper. Int. J. Biol. Macromol. 162, 1566–1577. https://doi.org/10.1016/j.ijbiomac.2020.08.035.
Bellamy, L.J., 1980. Alkanes. In: Bellamy, L.J. (Ed.), The Infrared Spectra of Complex Molecules. Springer Netherlands, Dordrecht, pp. 1–23. https://doi.org/10.1007/978-94-011-6520-4_1.
Benítez, J.J., Castillo, P.M., del Río, J.C., León-Camacho, M., Domínguez, E., Heredia, A., Guzmán-Puyol, S., Athanassiou, A., Heredia-Guerrero, J.A., 2018. Valorization of tomato processing by-products: fatty acid extraction and production of bio-based materials. Materials 11, 2211. https://doi.org/10.3390/ma11112211.
Benítez, J.J., Osbild, S., Guzman-Puyol, S., Heredia, A., Heredia-Guerrero, J.A., 2020. Bio-based coatings for food metal packaging inspired in biopolyester plant cutin. Polymers 12, 942. https://doi.org/10.3390/POLYM12040942.
Boccia, F., Di Donato, P., Covino, D., Poli, A., 2019. Food waste and bio-economy: a scenario for the Italian tomato market. J. Clean. Prod. 227, 424–433. https://doi.org/10.1016/j.jclepro.2019.04.180.
Bomgardner, M.M., 2013. No easy fix for food can coatings. Chem. Eng. News Arch. 91, 24–25. https://doi.org/10.1021/cen-09106-bus2.
Caldona, E.B., Smith, D.W., Wipf, D.O., 2020. Protective action of semi-fluorinated perfluorocyclobutyl polymer coatings against corrosion of mild steel. J. Mater. Sci. 55, 1796–1812. https://doi.org/10.1007/s10853-019-04025-2.
Commission, J.E., 2012. Characterisation Factors of the ILCD Recommended Life Cycle Impact Assessment Methods, Recommendations for Life Cycle Impact Assessment in the European Context - Based on Existing Environmental Impact Assessment Models and Factors? (EC-JRC, 2011). https://doi.org/10.2788/60825.
Cuccolini, S., Aldini, A., Visai, L., Daglia, M., Ferrari, D., 2013. Environmentally friendly lycopene purification from tomato peel waste: enzymatic assisted aqueous extraction. J. Agric. Food Chem. 61, 1646–1651. https://doi.org/10.1021/jf3027815.
Debeaufort, F., 2021. Metal Packaging, Packaging Materials and Processing for Food, Pharmaceuticals and Cosmetics. John Wiley & Sons, Inc., Hoboken, NJ, USA.
Deng, X., Herranz, T., Weis, C., Bluhm, H., Salmeron, M., 2008. Adsorption of water on Cu2O and Al2O3 thin films. J. Phys. Chem. C 112, 9668–9672. https://doi.org/10.1021/jp800944r.
Deshwal, G.K., Panjagari, N.R., 2020. Review on metal packaging: materials, forms, food applications, safety and recyclability. J. Food Sci. Technol. 57, 2377–2392. https://doi.org/10.1007/s13197-019-04172-z.
ECHEMI, 2021. The Current Situation and Future of Bisphenol A Industry [WWW Document]. URL. https://www.echemi.com/cms/410078.html.
El hadad, A.A., García-Galván, F.R., Mezour, M.A., Hickman, G.J., Soliman, I.E., Jiménez-Morales, A., Barranco, V., Galván, J.C., Perry, C.C., 2020. Organic-inorganic hybrid coatings containing phosphorus precursors prepared by sol–gel on Ti6Al4V alloy: electrochemical and in-vitro biocompatibility evaluation. Prog. Org. Coating 148, 105834. https://doi.org/10.1016/j.porgcoat.2020.105834.
Escórcio, R., Bento, A., Tomé, A.S., Correia, V.G., Rodrigues, R., Moreira, C.J.S., Marion, D., Bakan, B., Silva Pereira, C., 2022. Finding a needle in a haystack: producing antimicrobial cutin-derived oligomers from tomato pomace. ACS Sustain. Chem. Eng. 10, 11415–11427. https://doi.org/10.1021/acssuschemeng.2c03437.
Fouyet, S., Olivier, E., Leproux, P., Dutot, M., Rat, P., 2021. Bisphenol A, Bisphenol F, and Bisphenol S: the Bad and the Ugly. Where Is the Good? Life. https://doi.org/10.3390/life11040314.
Fragni, R., Zurlini, C., Montanari, A., Kiroplastis, V., Peñalba, F., 2006. Adhesion improvement of the UV lacquers for food cans by applying a post-curing current treatment. Prog. Org. Coating 55, 254–261. https://doi.org/10.1016/j.porgcoat.2005.11.009.
Grassino, A.N., Halambek, J., Djaković, S., Rimac Brnčić, S., Dent, M., Grabarić, Z., 2016. Utilization of tomato peel waste from canning factory as a potential source for pectin production and application as tin corrosion inhibitor. Food Hydrocolloids 52, 265–274. https://doi.org/10.1016/j.foodhyd.2015.06.020.
Guzmán-Puyol, S., Heredia, A., Heredia-Guerrero, J.A., Benítez, J.J., 2021. Cutin-Inspired polymers and plant cuticle-like composites as sustainable food packaging materials. In: Sustainable Food Packaging Technology. Wiley, pp. 161–198. https://doi.org/10.1002/9783527820078.ch6.
Hamzah, M.A.A.M., Hasham, R., Malek, N.A.N.N., Hashim, Z., Yahayu, M., Razak, F.I.A., Zakaria, Z.A., 2022. Beyond conventional biomass valorisation: pyrolysis-derived products for biomedical applications. Biofuel Res. J. 9, 1648–1658. https://doi.org/10.18331/BRJ2022.9.3.2.
Heredia-Guerrero, J.A., Caputo, G., Guzman-Puyol, S., Tedeschi, G., Heredia, A., Ceseracciu, L., Benitez, J.J., Athanassiou, A., 2019. Sustainable polycondensation of multifunctional fatty acids from tomato pomace agro-waste catalyzed by tin (II) 2-ethylhexanoate. Mater. Today Sustain. 3–4, 100004 https://doi.org/10.1016/j.mtsust.2018.12.001.
Heredia-Guerrero, J.A., Heredia, A., Domínguez, E., Cingolani, R., Bayer, I.S., Athanassiou, A., Benítez, J.J., 2017. Cutin from agro-waste as a raw material for the production of bioplastics. J. Exp. Bot. 68, 5401–5410. https://doi.org/10.1093/jxb/erx272.
Irvine, J.T.S., Sinclair, D.C., West, A.R., 1990. Electroceramics: characterization by impedance spectroscopy. Adv. Mater. 2, 132–138. https://doi.org/10.1002/adma.19900020304.
ISO 14044, 2006. Environmental Management – Life Cycle Assessment – Requirements and Guidelines, 2006.
Lu, Z., Wang, J., Gao, R., Ye, F., Zhao, G., 2019. Sustainable valorisation of tomato pomace: a comprehensive review. Trends Food Sci. Technol. 86, 172–187. https://doi.org/10.1016/j.tifs.2019.02.020.
Ma, S., Li, T., Liu, X., Zhu, J., 2016. Research progress on bio-based thermosetting resins. Polym. Int. 65, 164–173. https://doi.org/10.1002/pi.5027.
Mansfeld, F., 1995. Use of electrochemical impedance spectroscopy for the study of corrosion protection by polymer coatings. J. Appl. Electrochem. 25, 187–202. https://doi.org/10.1007/BF00262955.
Maraveas, C., 2020. Production of Sustainable and Biodegradable Polymers from Agricultural Waste. Polym. https://doi.org/10.3390/polym12051127.
Mirabedini, S.M., Arabi, H., Salem, A., Asiaban, S., 2007. Effect of low-pressure O2 and Ar plasma treatments on the wettability and morphology of biaxial-oriented polypropylene (BOPP) film. Prog. Org. Coating 60, 105–111. https://doi.org/10.1016/j.porgcoat.2007.07.007.
Morselli, D., Cataldi, P., Paul, U.C., Ceseracciu, L., Benitez, J.J., Scarpellini, A., Guzman-Puyol, S., Heredia, A., Valentini, P., Pompa, P.P., Marrero-López, D., Athanassiou, A., Heredia-Guerrero, J.A., 2021. Zinc polyaleuritate ionomer coatings as a sustainable, alternative technology for bisphenol A-free metal packaging. ACS Sustain. Chem. Eng. 9, 15484–15495. https://doi.org/10.1021/acssuschemeng.1c04815.
Namir, M., Siliha, H., Ramadan, M.F., 2015. Fiber pectin from tomato pomace: characteristics, functional properties and application in low-fat beef burger. J. Food Meas. Char. 9, 305–312. https://doi.org/10.1007/s11694-015-9236-5.
Nguyen, H., Jamali Moghadam, M., Moayedi, H., 2019. Agricultural wastes preparation, management, and applications in civil engineering: a review. J. Mater. Cycles Waste Manag. 21, 1039–1051. https://doi.org/10.1007/s10163-019-00872-y.
Otoni, C.G., Azeredo, H.M.C., Mattos, B.D., Beaumont, M., Correa, D.S., Rojas, O.J., 2021. The food–materials nexus: next generation bioplastics and advanced materials from agri-food residues. Adv. Mater. 33, 2102520 https://doi.org/10.1002/adma.202102520.
Owens, D.K., Wendt, R.C., 1969. Estimation of the surface free energy of polymers. J. Appl. Polym. Sci. 13, 1741–1747. https://doi.org/10.1002/app.1969.070130815.
Pajarito, B.B., Caguntas, A.J.F., Felices, N.B., Tubalinal, H.O.S., Leuterio, G.L.D., 2018. Corrosion, wettability, and adhesion of acrylic coatings containing silane-treated mineral fillers on carbon steel. Mater. Sci. Forum 917 MSF 252–256. https://doi.org/10.4028/www.scientific.net/MSF.917.252.
Pham, H.Q., Marks, M.J., 2005. Epoxy resins. In: Ullmann's Encyclopedia of Industrial Chemistry. https://doi.org/10.1002/14356007.a09_547.pub2.
Pilch-Pitera, B., 2014. Polyurethane powder coatings containing polysiloxane. Prog. Org. Coating 77, 1653–1662. https://doi.org/10.1016/j.porgcoat.2014.05.021.
Pirozzi, A., Ferrari, G., Donsì, F., 2022. Cellulose isolation from tomato pomace pretreated by high-pressure homogenization. Foods. https://doi.org/10.3390/foods11030266.
PlasticsEurope, 2022. What is BPA? [WWW Document]. URL. https://bisphenol-a-europe.org/what-is-bpa/.
PlasticsEurope, 2021. Plastics – the Facts 2021. An analysis of European plastics production, demand and waste data. Plast. Eur. Assoc. Plast. Manuf. 1–34.
Prokop, Z., Hanková, L., Jeřábek, K., 2004. Bisphenol A synthesis - modeling of industrial reactor and catalyst deactivation. React. Funct. Polym. 60, 77–83. https://doi.org/10.1016/j.reactfunctpolym.2004.02.013.
Silva, Y.P.A., Borba, B.C., Pereira, V.A., Reis, M.G., Caliari, M., Brooks, M.S.L., Ferreira, T.A.P.C., 2019. Characterization of tomato processing by-product for use as a potential functional food ingredient: nutritional composition, antioxidant activity and bioactive compounds. Int. J. Food Sci. Nutr. 70, 150–160. https://doi.org/10.1080/09637486.2018.1489530.
Simal-Gándara, J., 1999. Selection of can coatings for different applications. Food Rev. Int. 15, 121–137. https://doi.org/10.1080/87559129909541180.
Snyder, R.G., Schachtschneider, J.H., 1963. Vibrational analysis of the n-paraffins-I. Assignments of infrared bands in the spectra of C3H8 through n-C19H40. Spectrochim. Acta 19, 85–116. https://doi.org/10.1016/0371-1951(63)80095-8.
Ström, G., Fredriksson, M., Stenius, P., 1987. Contact angles, work of adhesion, and interfacial tensions at a dissolving Hydrocarbon surface. J. Colloid Interface Sci. 119, 352–361. https://doi.org/10.1016/0021-9797(87)90280-3.
Tassinari, R., Narciso, L., Tait, S., Busani, L., Martinelli, A., Di Virgilio, A., Carli, F., Deodati, A., La Rocca, C., Maranghi, F., 2020. Juvenile toxicity rodent model to study toxicological effects of bisphenol A (BPA) at dose levels derived from Italian children biomonitoring study. Toxicol. Sci. 173, 387–401. https://doi.org/10.1093/toxsci/kfz226.
Tedeschi, G., Guzman-Puyol, S., Ceseracciu, L., Benitez, J.J., Cataldi, P., Bissett, M., Heredia, A., Athanassiou, A., Heredia-Guerrero, J.A., 2020. Sustainable, high-barrier polyaleuritate/nanocellulose biocomposites. ACS Sustain. Chem. Eng. 8, 10682–10690. https://doi.org/10.1021/acssuschemeng.0c00909.
Tedeschi, G., Guzman-Puyol, S., Paul, U.C., Barthel, M.J., Goldoni, L., Caputo, G., Ceseracciu, L., Athanassiou, A., Heredia-Guerrero, J.A., 2018. Thermoplastic cellulose acetate oleate films with high barrier properties and ductile behaviour. Chem. Eng. J. 348, 840–849. https://doi.org/10.1016/j.cej.2018.05.031.
Tsang, Y.F., Kumar, V., Samadar, P., Yang, Y., Lee, J., Ok, Y.S., Song, H., Kim, K.-H., Kwon, E.E., Jeon, Y.J., 2019. Production of bioplastic through food waste valorization. Environ. Int. 127, 625–644. https://doi.org/10.1016/j.envint.2019.03.076.
Ulaeto, S.B., Mathew, G.M., Pancrecious, J.K., Rajimol, P.R., Karun, A.S., Rajan, T.P.D., 2023. Azadirachta indica (Neem) self-healing efficacy assessment in epoxy primer

coatings: a bio-responsive strategy for counteracting corrosion. Colloids Surf. A Physicochem. Eng. Asp. 658, 130684. https://doi.org/10.1016/j.colsurfa.2022.130684.

UNI EN ISO 14040, 2006. Environmental Management – Life Cycle Assessment – Principles and Framework, 2006.

Upadhyay, V., Battocchi, D., 2016. Localized electrochemical characterization of organic coatings: a brief review. Prog. Org. Coating 99, 365–377. https://doi.org/10.1016/j.porgcoat.2016.06.012.

van der Hulst, M.K., Huijbregts, M.A.J., van Loon, N., Theelen, M., Kootstra, L., Bergesen, J.D., Hauck, M., 2020. A systematic approach to assess the environmental impact of emerging technologies: a case study for the GHG footprint of CIGS solar photovoltaic laminate. J. Ind. Ecol. 24, 1234–1249. https://doi.org/10.1111/jiec.13027.

Vasyliev, G., Lyudmyla, K., Hladun, K., Skiba, M., Vorobyova, V., 2022. Valorization of tomato pomace: extraction of value-added components by deep eutectic solvents and their application in the formulation of cosmetic emulsions. Biomass Convers. Biorefinery 12, 95–111. https://doi.org/10.1007/s13399-022-02337-z.

Vorobyova, V., Skiba, M., 2022. Potential of tomato pomace extract as a multifunction inhibitor corrosion of mild steel. Waste and Biomass Valorization 13, 3309–3333. https://doi.org/10.1007/s12649-022-01715-y.

Westerdahl, C.A.L., Hall, J.R., Schramm, E.C., Levi, D.W., 1974. Gas plasma effects on polymer surfaces. J. Colloid Interface Sci. 47, 610–620. https://doi.org/10.1016/0021-9797(74)90238-0.

Zampori, L., Pant, R., 2019. Suggestions for updating the product environmental footprint (PEF) method, eur 29682 en. https://doi.org/10.2760/424613.

Zhang, W., Fan, X., Gu, X., Gong, S., Wu, J., Wang, Z., Wang, Q., Wang, S., 2020. Emulsifying properties of pectic polysaccharides obtained by sequential extraction from black tomato pomace. Food Hydrocolloids 100, 105454. https://doi.org/10.1016/j.foodhyd.2019.105454.